

# Method for Estimating the Wavenumber of Standing Waves Using Three Langmuir Probes

Tatsuya KOBAYASHI, Yoshihiko NAGASHIMA<sup>1)</sup>, Shigeru INAGAKI<sup>2)</sup>, Hiroyuki ARAKAWA, Makoto SASAKI<sup>2)</sup>, Takuma YAMADA<sup>1)</sup>, Masatoshi YAGI<sup>2)</sup>, Naohiro KASUYA<sup>3)</sup>, Akihide FUJISAWA<sup>2)</sup>, Sanae-I. ITOH<sup>2)</sup> and Kimitaka ITOH<sup>3)</sup>

*Interdisciplinary Graduate School of Engineering Sciences, Kyushu University, Fukuoka 816-8580, Japan*

<sup>1)</sup>*Graduate School of Frontier Sciences, The University of Tokyo, Tokyo 277-8561, Japan*

<sup>2)</sup>*Research Institute for Applied Mechanics, Kyushu University, Fukuoka 816-8580, Japan*

<sup>3)</sup>*National Institute for Fusion Science, Toki 509-5292, Japan*

(Received 5 January 2011 / Accepted 25 April 2011)

A new method for estimating the wavenumber of a standing wave system by using three Langmuir probes is proposed. Analytical formulae are derived from a simple model in which two waves of the same frequency and the same wavenumber propagate in opposite directions. The proposed method can estimate the wavenumber correctly even if the two waves have equal amplitude.

© 2011 The Japan Society of Plasma Science and Nuclear Fusion Research

Keywords: drift wave, standing wave, Langmuir probe, wavenumber measurement, cross phase

DOI: 10.1585/pfr.6.1401050

## 1. Introduction

An understanding of the mechanisms that form turbulent structure in magnetized plasma [1, 2] is important for reducing turbulence-driven transport. Much effort has been made to observe the spatio-temporal structure of fluctuations. Fluctuations azimuthally propagating in the electron and ion diamagnetic directions can coexist in a plasma. When two waves of the same frequency propagate in opposite directions, a standing wave can arise as a result of the interference between them. The standing wave appears in the edge region of the plasma because of wave reflection at the plasma boundary. In addition, zonal flows oscillate as a standing wave in the radial direction [3–7]. The conventional two-point measurement cannot identify a standing wave in principle. A multi-point simultaneous measurement, such as that by a 64-channel Langmuir probe array [8, 9], can detect fluctuations with various wavenumbers even if they include standing waves. However, multi-point measurement is not always realized because of its accessibility to plasmas. In this report, we propose a convenient new method for estimating the wavenumber in a standing wave system by using the least number of fluctuation measurements. Detection of standing waves can lead to a better understanding of the spatial structure of fluctuations and its nonlinear coupling in wavenumber space [10]. The new method is validated by test data, and its limitations are discussed.

## 2. Three-Point Measurement

We propose a three-point measurement aligned along

author's e-mail: kobayashi@riam.kyushu-u.ac.jp

the wave propagation direction. We consider a one-dimensional standing wave system in which two waves propagating in the  $+x$  and  $-x$  directions are called the forward and backward waves, respectively. The amplitude of the propagating waves is written as,

$$\begin{aligned} \psi(x, t) = & A_f \cos(\omega t - kx - \phi_f) \\ & + A_b \cos(\omega t + kx - \phi_b), \end{aligned} \quad (1)$$

where  $x$  and  $t$  are the position and time, respectively. The wave propagates with the wavenumber  $\pm k$  and oscillates with an angular frequency  $\omega$ , and  $A_f, A_b$  and  $\phi_f, \phi_b$  represent the amplitude and initial phase of each wave, respectively. The variables  $x, t, k$ , and  $\omega$  are nondimensional and can have arbitrary units. A standing wave appears when  $A_f, A_b \neq 0$ . The values of  $k, A_f$ , and  $A_b$  determine the spatial characteristics of the standing wave. The values of  $\phi_f$  and  $\phi_b$  determine the locations of nodes and antinodes, respectively. Here, we aim to estimate  $k, A_f$ , and  $A_b$ .

The waves observed at each probe position  $x_l$  are given as

$$\psi(x_l, t) = \Psi_l \cos(\omega t - \theta_l), l = 1, 2, 3, \quad (2)$$

where  $\Psi_l$  is the amplitude of the wave at each probe (obtained from the auto power spectrum  $S_l$  as  $\Psi_l^2 \propto S_l$ ), and  $\theta_l$  is the initial phase. The measurement setup and the typical test fluctuation field are shown in Fig. 1. Here, the test data contains white Gaussian noise. When three probes are aligned at the same interval  $\Delta x$ , Eqs. (1) and (2) yield the phase relationship among them, as below:

$$\Psi_1 \sin \Delta\theta_{12} = \Psi_3 \sin \Delta\theta_{23}, \quad (3)$$

where  $\Delta\theta_{lm}$  is the cross phase between two probes indicated by subscripts  $l$  and  $m$ . The wavenumber is derived as

$$\cos k\Delta x = \frac{\Psi_1 \cos \Delta\theta_{12} + \Psi_3 \cos \Delta\theta_{23}}{2\Psi_2}. \quad (4)$$

The amplitudes of the two waves are written as

$$A_f^2 = \frac{\Psi_1^2 + \Psi_2^2 - 2\Psi_1\Psi_2 \cos(k\Delta x - \Delta\theta_{12})}{4 \sin^2 k\Delta x} \quad (5)$$

and

$$A_b^2 = \frac{\Psi_1^2 + \Psi_2^2 - 2\Psi_1\Psi_2 \cos(k\Delta x + \Delta\theta_{12})}{4 \sin^2 k\Delta x}. \quad (6)$$

We can thus estimate  $k$ ,  $A_f$ , and  $A_b$  from  $\Psi_1$ ,  $\Psi_2$ ,  $\Psi_3$ ,  $\Delta\theta_{12}$ , and  $\Delta\theta_{23}$ , which can be obtained using spectrum analysis for each probe. In the simplest case  $R = A_b/A_f = 0$  (i.e. a pure propagating wave), conditions  $A_f = \Psi_1 = \Psi_2 = \Psi_3$  and  $\Delta\theta_{12} = \Delta\theta_{23}$  are satisfied. Using these conditions, Eq. (4) yields  $k = \Delta\theta_{12}/\Delta x$ . This is identical to the alignment used to estimate the wavenumber by the two-point

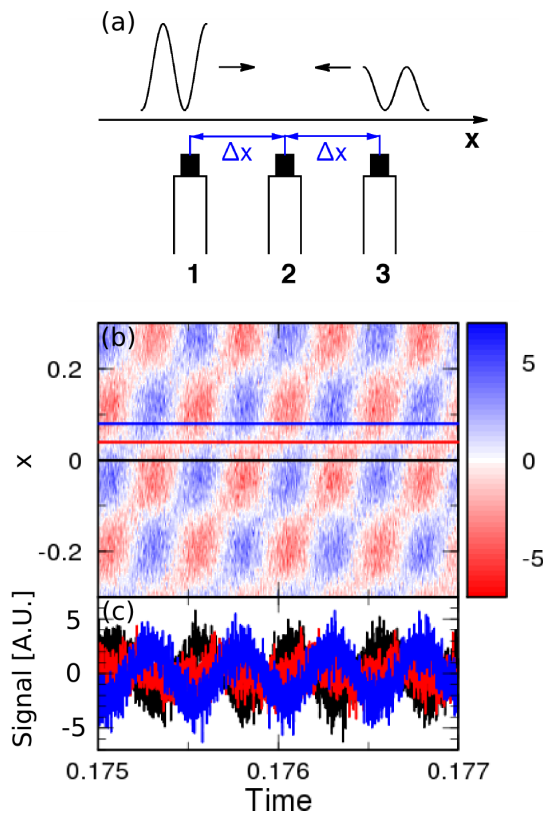


Fig. 1 (a) Typical configuration of three probes, (b) contour of test data for standing wave system, and (c) time evolution data from the three probes. Frequency of  $f = 2.0$  ( $f = \omega/2\pi$ ), wavenumber of  $k = 20$ , and amplitude ratio of  $R = A_f/A_b = 0.6$  are given. Initial phase difference is given as  $\phi_f - \phi_b = \pi/2$ . White Gaussian noise with a signal-to-noise (S/N) ratio (defined by the fluctuation power rate of signal to noise) of 500 is added. Three probes are fixed at  $x = 0, 0.04$ , and  $0.08$ .

measurement. Another simple case is  $R = 1$  (i.e. a pure standing wave). Using a condition of  $\Delta\theta_{12} = \Delta\theta_{23} = 0$ , Eq. (4) can be written as  $\cos k\Delta x = (\Psi_1 + \Psi_3)/2\Psi_2$ .

### 3. Tests of the Method

We checked the validity of our method using test data. The wavenumber  $k_{\text{test}}$ , the amplitude ratio  $R_{\text{test}} = A_b/A_f$ , and the signal-to-noise (S/N) ratio of the test data were varied. The probe spacing  $\Delta x$  was also varied. First, we applied our method to the simplest cases,  $R_{\text{test}} = 0.0$  and  $1.0$ ; the results are shown in Fig. 2 (a). In the region of  $\Delta x > \lambda_{\text{test}}/2$ , wavenumber estimation failed because  $\lambda_{\text{test}}$  was smaller than the spatial resolution of this probe system. The wavenumber was correctly estimated in both the cases. A relatively large error appeared for the case  $R_{\text{test}} = 1.0$ ,  $2\Delta x = 0.5\lambda$ , where one of the nodes of the standing wave was located at a probe position. In experiments, the node seldom appears because the condition of  $0.0 < R < 1.0$  is most likely to be obtained. Our method provided a correct  $k$  value even when  $k$  and  $R$  were varied over wide ranges, as shown in Figs. 2 (b) and (c).

Figure 3 shows the effect of noise for the estimated value of  $k$ . A larger wavenumber is estimated when the S/N ratio is small for  $2\Delta x/\lambda_{\text{test}} = 0.255$ . On the other hand,

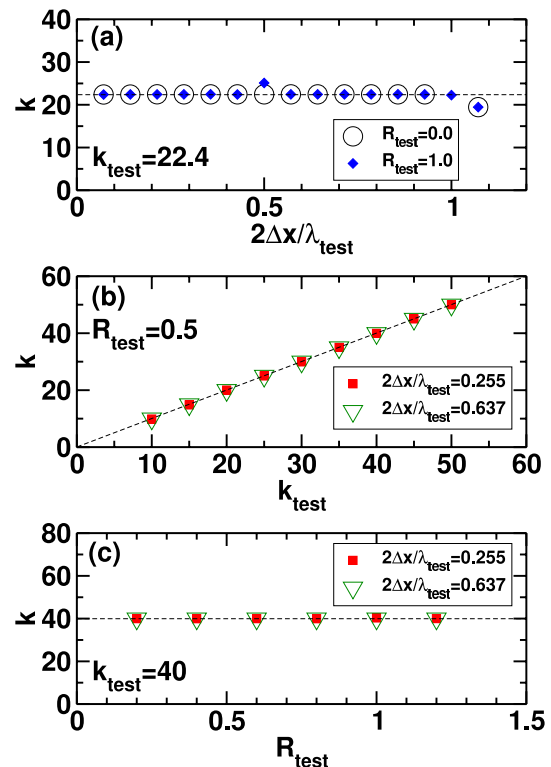


Fig. 2 Results of tests of the proposed method in the simplest cases, (a)  $R_{\text{test}} = 0.0$  and  $1.0$ , where Fourier transform analysis is applied using a time window of 2.00, and 30 time ensembles are averaged. Numerical stability of the proposed method with respect to (b)  $k$  and (c)  $R$ . White Gaussian noise with S/N ratio of 500 is added in all tests.

the estimated wavenumber is almost correct even if the S/N ratio is small for  $2\Delta x/\lambda_{\text{test}} = 0.509$  and  $0.764$ . The appropriate probe spacing is limited when the S/N ratio is small, that is, when  $S/N < 0.1$ .

To determine the cause of the estimation error (i.e. a larger wavenumber is estimated when the S/N ratio is small in Fig. 3), we show each term in Eq. (4) ( $\Psi_1$ ,  $\Psi_2$ ,  $\Psi_3$ ,  $\Delta\theta_{12}$ , and  $\Delta\theta_{23}$ ) as a function of the S/N ratio. Figures 4 (a) and (b) show  $\Psi_1$ ,  $\Psi_2$ , and  $\Psi_3$ , and Figs. 4 (c) and (d) show  $\Delta\theta_{12}$  and  $\Delta\theta_{23}$  (error bars represent the standard deviations of the cross phase). In these figures, the left and right columns

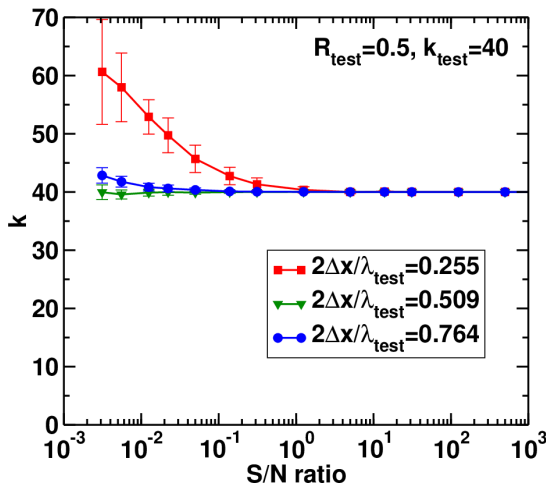


Fig. 3 Estimated wavenumbers as a function of S/N ratio, where  $k_{\text{test}} = 40$  and  $R_{\text{test}} = 0.5$ . Time window and the number of ensembles are 0.50 and 240, respectively. The wavenumber error bar is the standard deviation of 60 estimation trials.

are the results of spectral analyses for  $2\Delta x/\lambda_{\text{test}} = 0.255$  (relatively large error) and  $0.509$  (relatively small error), respectively. The pair of fluctuation power ratios  $\Psi_1^2/\Psi_2^2$  and  $\Psi_3^2/\Psi_2^2$  are not constant since the S/N ratio decreases when  $2\Delta x/\lambda_{\text{test}} = 0.255$ . The pair of fluctuation power ratios is constant when  $2\Delta x/\lambda_{\text{test}} = 0.509$ . This difference in the fluctuation power ratios causes the difference in the errors between these two conditions. When the signal fluctuation powers from the three probes are not similar, the fluctuation ratios can be affected by the offset of the fluctuation power due to noise. Therefore, it becomes difficult to estimate the correct wavenumber when the noise amplitude is comparable to the signal amplitude. This error is systematic and is difficult to reduce by increasing the statistical accuracy (e.g., increasing the ensemble number). The shape of the noise spectrum also affects this estimation error in the case of non-white noise. For example, pink noise, which has the power spectrum density proportional to the inverse of the frequency, has a greater effect on the wavenumber estimation of low-frequency waves. On the other hand, the cross phases in both cases (Figs. 4 (c) and (d)) are constant as the S/N ratio decreases. The error bars of the cross phases increase with the decreasing S/N ratio. Therefore, the error bars are larger in the smaller S/N ratio regime.

## 4. Discussion

Experimental results show that waves with the same frequency but different wavenumbers exist in magnetized plasmas. We discuss the effect of such waves on estimation of  $k$  value by applying our method. A wave defined as

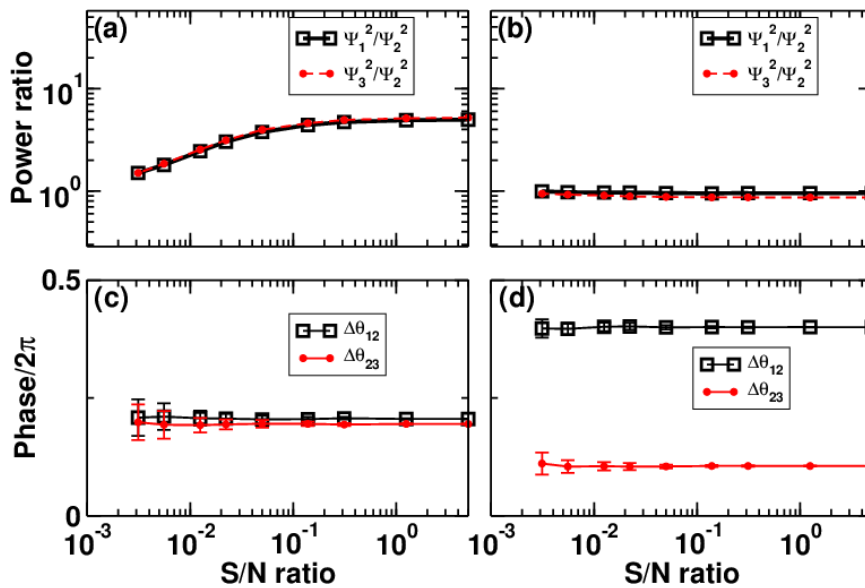


Fig. 4 Results of spectral analysis of test data used in Fig. 3 as a function of S/N ratio. (a), (b) Fluctuating power ratios  $\Psi_1^2/\Psi_2^2$  and  $\Psi_3^2/\Psi_2^2$  for  $2\Delta x/\lambda_{\text{test}} = 0.255$  and  $2\Delta x/\lambda_{\text{test}} = 0.509$ , respectively. (c), (d) Cross phases  $\Delta\theta_{12}$  and  $\Delta\theta_{23}$  for  $2\Delta x/\lambda_{\text{test}} = 0.255$  and  $2\Delta x/\lambda_{\text{test}} = 0.509$ , respectively.

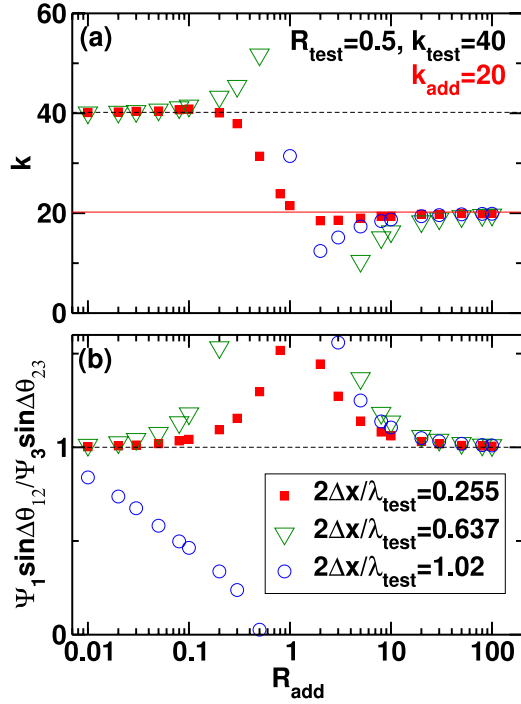


Fig. 5 Results of the proposed method for test data including an additional wave. (a) Estimated wavenumber and (b)  $\Psi_1 \sin \Delta\theta_{12} / \Psi_3 \sin \Delta\theta_{23}$  as a function of  $R_{\text{add}}$ . Black dashed line and red solid line indicate  $k = 40$  and  $k = 20$ , respectively. Time window of 2.00 and 30 ensembles are used for fast Fourier transform.

$$\psi(x, t) = A_{\text{add}} \cos(\omega t - k_{\text{add}}x - \phi_{\text{add}}) \quad (7)$$

is added to the test data. The additional wave contamination ratio is defined as  $R_{\text{add}} = A_{\text{add}}/A_f$ . Figure 5(a) shows the results of our method when such contamination is present. When the amplitude of the additional wave is small ( $R_{\text{add}} < 0.1$ ), estimation is successful. In contrast, when the amplitude of the additional wave is comparable to that of the target standing wave ( $R_{\text{add}} \sim 1.0$ ), the proposed method cannot provide the correct value. In addition, when the amplitude of the additional wave is much larger than that of the standing wave ( $R_{\text{add}} > 10$ ), the wavenumber of the additional wave ( $k_{\text{add}} = 20$ ) can be estimated. Three types of probe distances were tested, which indicate similar tendencies, i.e.,  $2\Delta x/\lambda_{\text{test}} = 1.02$  is out of range for  $k$ ; however,  $2\Delta x/\lambda_{\text{add}} = 0.51$  is within the limit of application for  $k_{\text{add}}$ . When the proposed method successfully estimates  $k$  ( $R_{\text{add}} \ll 0.1$  or  $R_{\text{add}} \gg 10$ ), Eq. (3) is satisfied, i.e.,  $\Psi_1 \sin \Delta\theta_{12} / \Psi_3 \sin \Delta\theta_{23} = 1$ . However, this relation is not satisfied in the range  $0.1 < R_{\text{add}} < 10$ , as shown in Fig. 5(b). Equation (3) can be used to check possible applications of the proposed method.

## 5. Summary

A new method for estimating the wavenumber and amplitudes of a standing wave system by using three-point

fluctuation measurement was proposed. Convenient formulae for estimation of the wavenumber (Eq. (4)) and amplitudes of forward and backward waves (Eqs. (5) and (6), respectively) were derived. The validity of the proposed method was tested using simulated data with white Gaussian noise. The formulae can be used if the S/N ratio is greater than 0.1 and the amplitude ratio of the standing wave and the additional wave is less than 0.1.

## Acknowledgments

This work was partly supported by a Grant-in-Aid for Scientific Research S from JSPS (21224014), a Grant-in-Aid for Scientific Research C from JSPS (20560767), the collaboration programs between RIAM Kyushu University and the NIFS (NIFS10KOAP023).

## Appendix

A detailed explanation of the derivation process is given by Eqs. (1) and (2). The expressions given by complex variables in Eqs. (1) and (2) are general:

$$\psi(x, t) = A_f e^{i(-\omega t + kx + \phi_f)} + A_b e^{i(-\omega t - kx + \phi_b)} \quad (A.1)$$

and

$$\psi((l-2)\Delta x, t) = \Psi_l e^{i(-\omega t + \theta_l)}, \quad l = 1, 2, 3, \text{ respectively,} \quad (A.2)$$

where the quantities  $A_f, A_b$  and  $\Psi_l$  are real, and  $x_2$  is defined as the origin. Comparing the imaginary parts of Eqs. (A.1) and (A.2) at  $x = 0$  ( $l = 2$ ) yields expressions for  $\Psi_2$  and  $\theta_2$  using  $A_f, A_b, \phi_f$ , and  $\phi_b$ :

$$\Psi_2^2 = A_f^2 + A_b^2 + 2A_f A_b \cos(\phi_f - \phi_b) \quad (A.3)$$

and

$$\tan \theta_2 = \frac{A_f \sin \phi_f + A_b \sin \phi_b}{A_f \cos \phi_f + A_b \cos \phi_b}, \quad (A.4)$$

respectively. Then, comparing Eqs. (A.1) and (A.2) at  $x = -\Delta x$  ( $l = 1$ ) and  $x = \Delta x$  ( $l = 3$ ) with those at  $x = 0$  ( $l = 2$ ), we obtain

$$\begin{aligned} A_f^2 e^{-ik\Delta x} + A_b^2 e^{ik\Delta x} + 2A_f A_b \cos(-k\Delta x + \phi_f - \phi_b) \\ = \Psi_2 \Psi_1 e^{i\Delta\theta_{12}} \end{aligned} \quad (A.5)$$

and

$$\begin{aligned} A_f^2 e^{ik\Delta x} + A_b^2 e^{-ik\Delta x} + 2A_f A_b \cos(k\Delta x + \phi_f - \phi_b) \\ = \Psi_2 \Psi_3 e^{-i\Delta\theta_{23}}, \end{aligned} \quad (A.6)$$

respectively. Summing Eqs. (A.5) and (A.6) and combining with Eq. (A.3) gives

$$2\Psi_2 \cos k\Delta x = \Psi_1 e^{i\Delta\theta_{12}} + \Psi_3 e^{-i\Delta\theta_{23}}. \quad (A.7)$$

One can obtain Eqs. (3) and (4) from Eq. (A.7) by comparing their imaginary and real parts, respectively. On the other hand, the real and imaginary parts of Eq. (A.5) are

$$\begin{aligned} \Psi_2^2 \cos k\Delta x + 2A_f A_b \sin k\Delta x \sin(\phi_f - \phi_b) \\ = \Psi_2 \Psi_1 \cos \Delta\theta_{12} \end{aligned} \quad (A.8)$$

and

$$-A_f^2 \sin k\Delta x + A_b^2 \sin k\Delta x = \Psi_2 \Psi_1 \sin \Delta\theta_{12}, \quad (\text{A.9})$$

respectively. Eliminating  $\phi_f - \phi_b$  from Eqs. (A.3), (A.8), and (A.9) gives

$$A_f^2 + A_b^2 = \frac{\Psi_1^2 + \Psi_2^2 - 2\Psi_1\Psi_2 \cos k\Delta x \cos \Delta\theta_{12}}{2 \sin^2 k\Delta x}. \quad (\text{A.10})$$

Equation (A.9) gives

$$A_f^2 - A_b^2 = -\frac{\Psi_1\Psi_2 \sin k\Delta x \sin \Delta\theta_{12}}{\sin^2 k\Delta x}. \quad (\text{A.11})$$

Equations (5) and (6) are derived from Eqs. (A.10) and

(A.11) by summing and subtracting, respectively.

- [1] P.H. Diamond *et al.*, Plasma Phys. Control. Fusion **47**, R35 (2005).
- [2] K. Itoh *et al.*, Phys. Plasmas **13**, 055502 (2007).
- [3] Y. Nagashima *et al.*, Phys. Plasmas **16**, 20706 (2009).
- [4] M. Sasaki *et al.*, Contrib. Plasma Phys. **48**, 68 (2008).
- [5] T. Ido *et al.*, Plasma Phys. Control. Fusion **48**, S41 (2006).
- [6] K. Hallatschek *et al.*, Phys. Rev. Lett. **86**, 1223 (2001).
- [7] N. Miyato *et al.*, Phys. Plasma **11**, 5557 (2004).
- [8] T. Yamada *et al.*, Rev. Sci. Instrum. **78**, 123501 (2007).
- [9] T. Yamada *et al.*, Nature Phys. **4**, 721 (2008).
- [10] M. Ramisch *et al.*, New J. Phys. **5**, 12.1 (2003).